ORIGINAL RESEARCH PAPER

An empirical significant duration relationship for stable continental regions

Jongwon Lee · Russell A. Green

Abstract An empirical predictive relationship correlating significant duration to earthquake magnitude, site-to-source distance, and local site conditions (i.e., rock vs. stiff soil) for stable continental regions is presented herein. The correlations were developed from data derived from 620 horizontal motions for stable continental regions (e.g., central and eastern North America: CENA), consisting of 28 recorded motions and 592 scaled motions. The data set encompasses the earthquake magnitude from 4.5 to 7.6 and the distance from 0.1 to 199 km. The non-linear mixed-effects regression technique was used to fit a predictive model to the significant duration data. Similar to the trend observed from active shallow crustal region motions, significant durations predicted for stable continental region motions increased with increasing earthquake magnitude and increasing site-to-source distance. In comparing the predicted durations for CENA motions with those for motions from active shallow crustal regions (e.g., western North America: WNA), it is shown that the differences in significant durations for the two regions are relatively minor for site-to-source distances less than about 100 km. Lastly, the significant durations predicted by the proposed model are shown to be in good agreement with durations of the motions recorded during the Mineral, Virginia earthquake of August 23, 2011.

J. Lee
Arup, 560 Mission Street Suite 700, San Francisco, CA 94105, USA
e-mail: jongwon.lee@arup.com

R. A. Green (✉)
Charles E. Via, Jr. Department of Civil and Environmental Engineering (MC 0105),
120B Patton Hall, Virginia Tech, 750 Drillfield Drive, Blacksburg, VA 24061, USA
e-mail: rugreen@vt.edu

1 Introduction

The objective of the study presented herein is the development of an empirical relationship correlating significant duration to earthquake magnitude, site-to-source distance, and local site conditions (i.e., rock vs. stiff soil) for stable continental regions (e.g., central/eastern North America: CENA). Strong ground motion duration is an important parameter for seismic risk assessment because it, along with the amplitude and frequency content of the ground motions, significantly influences the response of geotechnical and structural systems. For example, when the non-linear behavior (i.e., degradation of stiffness) of a system is considered, strong motion duration is a critical feature influencing the amount of damage that will occur (e.g., Bommer and Martinez-Pereira 1999). In this vein, various definitions of duration have been proposed for quantifying the strong motion phase of earthquake ground shakings, which is the portion of the motion that is of engineering interest.

Significant duration is one of the most frequently used definitions by engineering seismologists and earthquake engineers. For example, U.S. Nuclear Regulatory Commission (NRC) requires ground motion time histories developed for seismic site response or structural analyses that be checked to ensure their significant durations are consistent with the characteristics of the controlling earthquake scenarios (U.S. Nuclear Regulatory Commission 2007). The normalized cumulative squared acceleration, $H(t)$, is used in its definition:

$$H(t) = \frac{\int_0^t a^2(t)dt}{\int_0^{t_d} a^2(t)dt} \qquad (1)$$

where: $a(t)$ is the ground motion acceleration time history, and t_d is the total duration of the acceleration time history. As may be surmised from this equation, the normalized cumulative squared acceleration varies from 0 to 1 (or 0 to 100 %). Significant duration is most often defined as the time interval between $H(t) = 5$ and 75 % (Somerville et al. 1997) or $H(t) = 5$ and 95 % (Trifunac and Brady 1975), denoted as D_{5-75} and D_{5-95}, respectively. Figure 1 illustrates the determination of the D_{5-75} and D_{5-95} for an acceleration time history using the $H(t)$ plot, commonly referred to as a Husid plot (Husid 1969). The significant duration is useful because it reasonably represents the duration of the most significant shaking, based on a relative criterion (Bommer and Martinez-Pereira 1999). Hence, when significant duration is used in seismic risk assessments, the amplitude of acceleration must also be considered (Kempton and Stewart 2006).

The empirical relationship presented herein correlates significant duration (i.e., D_{5-75} and D_{5-95}) to earthquake magnitude, site-to-source distance, and local site conditions (i.e., rock vs. stiff soil) for stable continental regions. It is noted that fault mechanism (e.g., normal vs. strike slip), mainshock/aftershock and geographical effects (e.g., basin effects) are not considered herein. This is because this study uses mostly scaled ground motion data for stable continental regions, not actual recorded data, and scaling procedure used is not refined enough to account for these effects. Also, the locations of most faults in the CENA are unknown, let alone fault mechanisms. Thus, a refined duration relationship that accounted for such effects would not necessarily result improved duration predictions, from a pragmatic implementation perspective.

The authors also present a similarly developed relationship for active shallow crustal regions (e.g., western North America: WNA). This WNA relationship was developed so that consistent comparisons in ground motion duration for the two regions could be made. Although there are existing relationships for significant duration for WNA, the authors felt that in order to avoid issues related to differences in predicted duration due to disparities in database size, analysis techniques, etc., consistently developed relationships for the two
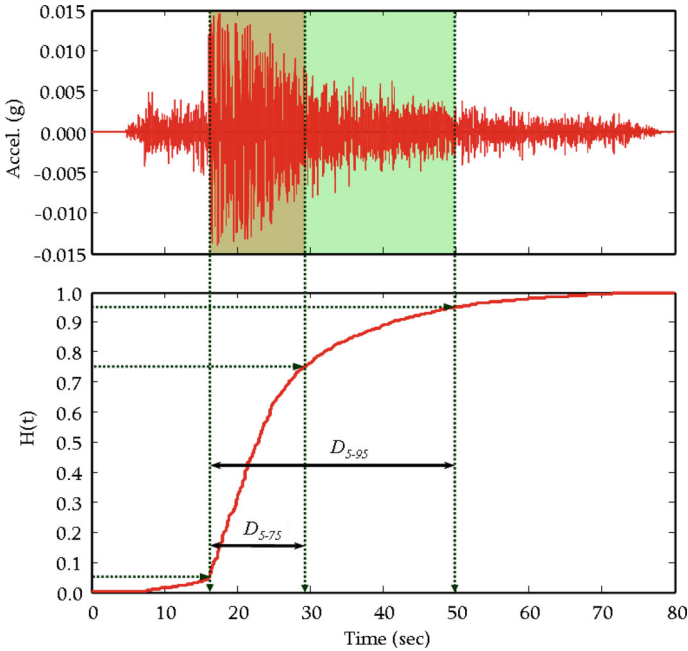
Fig. 1 Signification duration determination using the Husid plot for a ground acceleration time history (1125A54E: M5.9; R91.4 km) from the 1988 Saguenay earthquake

regions were needed to make valid comparisons. The correlations were developed by performing non-linear mixed-effects (NLME) regression analyses on data derived from 648 horizontal motion recordings for active shallow crustal regions (e.g., WNA), and 620 horizontal motions for stable continental regions (e.g., CENA). The latter ground motion dataset was comprised of both recorded motions and scaled motions and is discussed in more detail later in the paper. [Note that the acronyms "CENA" and "WNA" in this paper are used for convenience to refer to "stable continental" and "active shallow crustal" regions, respectively. However, the authors contend that the use of these respective relationships are not solely limited to North America, but rather are applicable for use in stable continental and active shallow tectonic regions in other parts of the world too.]

Regarding the organization of this paper, first the strong ground motion database used in this study is described. Then, basic concepts of the NLME regression method are reviewed, and the proposed functional form of the predictive model is introduced. Next, the results of the regression analyses and a comparison of significant durations predicted by this study's empirical relationships for stable continental and active shallow crustal regions are presented. A comparison of this study's relationship to existing relationships for active shallow crustal regions is then presented. Additionally, the significant durations of the recent 2011 Mineral, Virginia earthquake motions are compared with the proposed model. The procedure used to scale the scaled CENA motions is summarized in the "Appendix".

2 Strong ground motion data

The data set used in this study consists of 324 three-component (i.e., one vertical and two horizontal) sets of strong ground motion time histories from WNA and 310 sets for CENA.
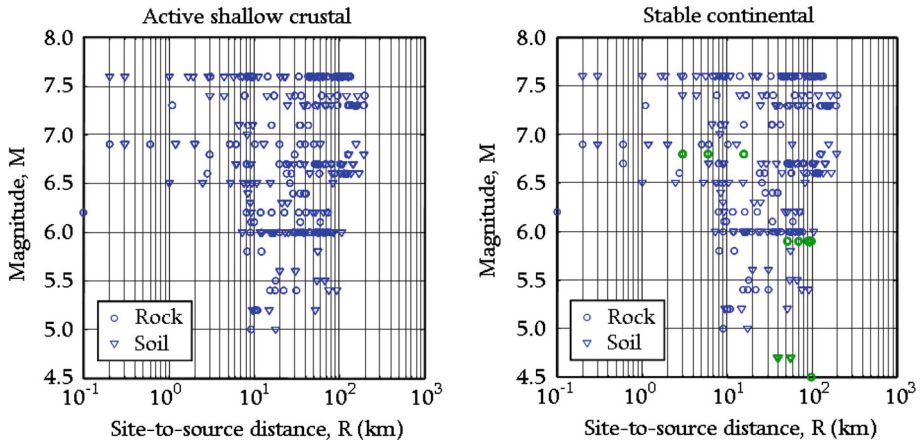
Fig. 2 Earthquake magnitude and site-to-source distance distributions (recorded motions for CENA are shown in *bold*)

Thus, a total of 648 and 620 horizontal time histories were used to develop the empirical relationships for WNA and CENA, respectively. This study adopted the ground motion dataset assembled by McGuire et al. (2001). Primarily, this dataset was intended to provide a library of strong ground motion time histories suitable for engineering analyses. The strong motion data for WNA were from 49 mainshock events, with the 1999 Chi–Chi earthquake being the most recent event included in the database. The moment magnitudes of these events range from 5.0 to 7.6, and the site-to-source distances range from 0.1 to 199.1 km, where site-to-source distance is defined as the closest distance to the fault rupture plane. Because there are few recorded strong ground motions in stable continental regions, only 28 of the motions in the CENA dataset are recorded motions, with the remaining 592 motions being "scaled" WNA motions for CENA conditions. A brief summary of the scaling procedure is provided below, with a more detail description of the scaling procedure given in the Appendix. The moment magnitudes for these motions range from 4.5 to 7.6, and the site-to-source distances range from 0.1 to 199.1 km. The recorded motions include the 1988 Saguenay (main shock M_w 5.9 and aftershock M_w 4.5), the 1985 Nahanni (M_w 6.8), and the 1989 New Madrid, MO (M_w 4.7) earthquakes. Figure 2 shows the magnitude and site-to-source distance distributions for both regions.

McGuire et al. (2001) scaled the WNA motions for CENA conditions using response spectral transfer functions generated from the single-corner frequency point source model in conjunction with random vibration theory (RVT) (e.g., Brune 1970, 1971; Boore 1983; McGuire et al. 2001; Silva and Lee 1987). The transfer functions account for the differences in seismic source, wave propagation path properties, and site effects between the WNA and CENA regions. Many seismological publications have shown successful results of the RVT point source model for generating strong ground motions for both WNA and CENA (Boore 1983, 1986; McGuire and Hanks 1980; McGuire et al. 1984; Schneider et al. 1993; Silva 1993;). In generating the scaled CENA motions, recorded WNA motions were used as "seed" motions in the spectral scaling process, resulting in scaled motions that have realistic characteristics. In this context, the stochastic point source model is a reliable and reasonable approach for estimating spectral characteristics of strong ground motions for engineering analyses. The scaling method however, should be verified as additional recordings of stable continental motions become available.

Table 1 Third letter: geotechnical subsurface characteristics of geomatrix 3-letter site classification

Third letter	Site description	Comments
A	Rock	Instrument on rock ($V_S > 600$ m/s) or <5 m of soil over rock
B	Shallow (stiff) soil	Instrument on/in soil profile up to 20 m thick overlying rock
C	Deep narrow soil	Instrument on/in soil profile at least 20 m thick overlying rock, in a narrow canyon or valley no more than several km wide
D	Deep broad soil	Instrument on/in soil profile at least 20 m thick overlying rock, in a broad valley
E	Soft deep soil	Instrument on/in deep soil profile with average $V_S < 150$ m/s

The ground motions were classified as either "rock" or "soil" based on the site conditions at the respective seismograph stations. The site classification scheme used by McGuire et al. (2001) is based on the third letter of the Geomatrix 3-letter site classification system shown in Table 1. Site categories A and B were considered to represent rock sites, and site categories C, D, and E were considered to represent soil sites (note that there were only a few motions in the McGuire et al. database that were recorded in category E sites).

3 Regression analyses

The regression analyses were performed on the significant durations of the individual horizontal components of the data set using the non-linear mixed-effects (NLME) regression technique. The NLME modeling is a maximum likelihood method based on normal (Gaussian) distribution and is primarily used for analyzing grouped data (i.e., databases comprised of subsets). The NLME regression method allows regression models to account for both random effects that vary from subset to subset and fixed-effects that do not. In this study, a subset consists of motions recorded during a given earthquake. In comparison to applying a fixed-effects regression technique (e.g., the least squares method) to the entire dataset, a mixed-effects regression method allows both inter- and intra-earthquake uncertainty to be quantified. This regression method produces unbiased fittings for each subset having different numbers of ground motion recordings. This is important because of the number of motions from each earthquake can widely vary.

NLME modeling estimates the variation in the mean values among earthquakes (i.e., inter-event variability) and the variation in the data for a single earthquake (i.e., intra-event variability) via the variances of inter-event errors and intra-event errors, respectively. The inter-event error is designated by η_i where the subscript, i represents the ith event (i.e., set of motions from a given earthquake). The inter-event error is defined as the difference between the median for the ith event and the median of the entire database (i.e., model median), and has a mean of zero and a variance of τ^2. The intra-event error is designated by ε_{ij} where the subscripts, ij indicate the jth record of the ith event. The intra-event error is defined as the difference between the data value of the jth record and the median for the ith event, and has a mean of zero and a variance of σ^2. The total error for the jth record of the ith event is defined as the sum of the corresponding inter- and intra-event errors (i.e., $\eta_i + \varepsilon_{ij}$). The standard deviation of the total error is given by:

$$\sigma_{total} = \sqrt{\tau^2 + \sigma^2} \tag{2}$$

where: σ_{total} is the standard deviation of total error, also called the total standard deviation. The NLME method assumes the normal distribution for intra-event errors and random-effects (Pinheiro and Bates 2000), which underlies the theoretical formulation of the NLME regression analyses. The inherent distributional assumptions are checked by the normal quantile–quantile (Q–Q), where the data points plotted approximately as a straight line indicates that the data is normally distributed. The statistical analysis program R (version 2.5.0) was used to perform the NLME regression analyses (Lee 2009; Pinheiro and Bates 2000).

4 Proposed model and regression results

The functional form of the predictive relationship used in this study is a variant of that proposed by Abrahamson and Silva (1996). In developing the functional form of their relationship, Abrahamson and Silva started with the seismic source duration relation (Boore 1983; Hanks 1979; McGuire and Hanks 1980):

$$D_0 = f_c^{-1} \tag{3}$$

where: D_0 is source duration, and f_c is the corner frequency, which separates the relatively-flat portion at intermediate frequencies in the Fourier amplitude spectrum from the decaying portion at low frequencies. The corner frequency is related to earthquake magnitude by the following relations:

$$f_c = 4.9 \times 10^6 \cdot \beta_0 \cdot (\Delta\sigma/M_0)^{1/3} \text{ (Brune 1970, 1971)} \tag{4}$$

$$\log M_0 = 1.5M + 16.05 \text{ (Hanks and Kanamori 1979)} \tag{5}$$

where: β_0 is shear wave velocity at the source (km/sec); $\Delta\sigma$ is stress drop at the source (bars); M_0 is seismic moment (dyne-cm); and M is moment magnitude.

Abrahamson and Silva (1996) modeled the magnitude dependence of $\Delta\sigma$ as:

$$\Delta\sigma (M) = \exp [b_1 + b_2 (M - 6)] \tag{6}$$

where, b_1 and b_2 are regression coefficients. Assuming a log-normal distribution for the significant duration data, Abrahamson and Silva (1996) proposed the following functional form for both D_{5-5} and D_{5-95}:

$$\ln D_{5-75} \text{ or } \ln D_{5-95} = \ln \left(\frac{\left(\frac{\Delta\sigma (M)}{10^{1.5M+16.05}} \right)^{-\frac{1}{3}}}{4.9 \times 10^6 \beta_0} + f_1(R) + f_2(M, R, S_S) \right) \tag{7}$$

where: R is site-to source distance (km); S_S is a binary parameter representing local site conditions (i.e., $S_S = 0$ for rock site; $S_S = 1$ for soil site); and $f_1(R)$ and $f_2(M\,R\,S_S)$ represent the site-to-source distance and local site condition dependences, respectively.

For the study presented herein, the first term inside the brackets on the right hand side of Eq. 7 (i.e., magnitude-β_0 term) was simplified to an exponential term for magnitude. This was done because the trends in the two terms were found to be very similar to each other, as shown in Fig. 3, where $b_1 = 5.20$; $b_2 = 0.85$; and $\beta_0 = 3.2$ km/s (Abrahamson and Silva 1996). It should be noted that the predictive model with this simplified term produced lower standard deviations than the model proposed by Abrahamson and Silva (1996) when fit to the same data.

Fig. 3 Comparison between the magnitude-β_0 term and an exponential term (C is a regression coefficient; $C = 1.86$ was used for this comparison)
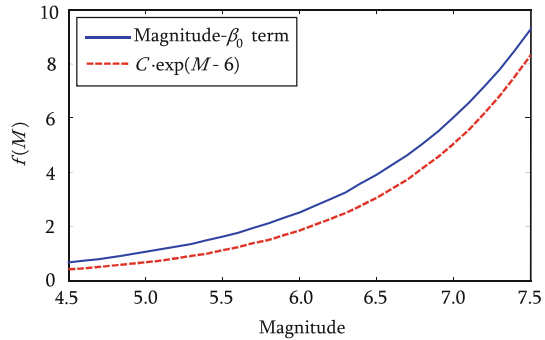

Table 2 Regression coefficients; p values (in parentheses); and standard deviations of inter-event, intra-event, and total errors

	C_1	C_2	C_3	S_1	S_2	S_3	τ_{ln}	σ_{ln}	$\sigma_{ln\,total}$
CENA									
D_{5-75}	0	2.23	0.10	−0.72	−0.19	−0.014	0.46	0.35	0.58
	(n/a)	(0.000)	(0.000)	(0.007)	(0.500)	(0.078)			
D_{5-95}	2.50	4.21	0.14	−0.98	−0.45	−0.0071	0.37	0.32	0.49
	(0.014)	(0.000)	(0.000)	(0.122)	(0.493)	(0.626)			
WNA									
D_{5-75}	0	1.86	0.06	0.22	0	0	0.28	0.37	0.46
	(n/a)	(0.000)	(0.000)	(0.165)	(n/a)	(n/a)			
D_{5-95}	1.50	3.22	0.11	2.01	0.80	−0.0097	0.26	0.28	0.38
	(0.010)	(0.000)	(0.000)	(0.000)	(0.094)	(0.341)			

Numerous regressions analyses were performed using various functional forms for the predictive relationships. However, based on observed trends in the data and the relative magnitude of the resulting standard deviations, the following functional form of the predictive relationship gave the best fit of the data:

$$\ln D_{5-75} \text{ or } \ln D_{5-95} = \ln \{C_1 + C_2 \exp(M - 6) + C_3 R + [S_1 + S_2(M - 6) + S_3 R]\, S_S\}$$

(8)

where, C_1 through C_3 and S_1 through S_3 are regression coefficients; M is the moment magnitude; R is the closest distance to the fault rupture plane (km); and S_S is a binary number representing local site conditions: $S_S = 0$ for rock sites and $S_S = 1$ for soil sites.

The standard deviations and p values from NLME regressions for D_{5-75} and D_{5-95} are listed in Table 2 for both CENA and WNA. The p value is a measure of the statistical significance of a regression coefficient in the model. A p value close to zero indicates that the corresponding regression coefficient has a significant statistical contribution. A p value of 5 % (i.e., 0.05) is typically considered the threshold for statistical significance (i.e., a coefficient with a p value smaller than 0.05 is statistically significant). For D_{5-75}, the coefficient C_1 was removed from the model because doing so resulted in a lower total standard deviation. Additionally, the coefficients S_2 and S_3 for WNA were also removed based on the total standard deviation and p values. It should be noted that in lieu of actually removing the terms from Eq. 8, the corresponding regression coefficients were just set equal to zero. This allowed
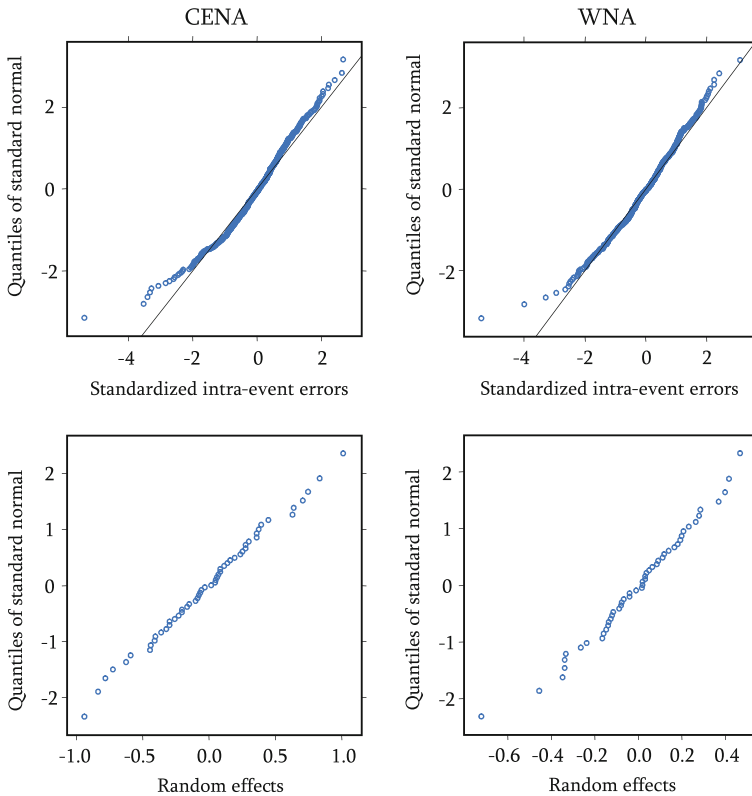
Fig. 4 Normal Q–Q plots of intra-event errors (*top*) and random-effects (*bottom*) for CENA (*left*) and WNA (*right*): D_{5-75}

the same functional form of the regression equation to be used for both D_{5-75} and D_{5-95}. Also, as shown in Table 2, other coefficients have *p* values greater than 5 % (i.e., 0.05), but it was decided to keep these coefficients in the proposed model since they were considered necessary to either lower the standard deviations or ensure valid physical interpretation of the data. Comparing the total standard deviations of the duration predictions for CENA and WNA motions, CENA appears to have larger standard deviations of the total errors than WNA for both D_{5-75} and D_{5-95}. This is mainly attributed to much larger variability quantified for different earthquakes for the CENA than those for the WNA. The total standard deviations for D_{5-95} are consistently smaller than those for D_{5-75}.

The distributional assumptions for intra-event errors and random-effects were assessed by the normal Q–Q plots shown in Figs. 4 and 5 for D_{5-75} and D_{5-95}, respectively. In these figures, the theoretical quantiles of the standard normal distribution versus the standardized intra-event errors (i.e., intra-event errors divided by their standard deviation) and random-effects are plotted. As shown in Figs. 4 and 5, both intra-event errors and random-effects follow normal distributions, consistent with the assumptions inherent to NLME modeling.

Using Eq. 8 in conjunction with the coefficients listed in Table 2, D_{5-75} and D_{5-95} medians for CENA are plotted in Figs. 6 and 7, respectively, as functions of site-to-source distance (*R*) for M5.5, M6.5, and M7.5 for both rock and soil sites. Similar to the trends observed from WNA motions by other investigators (e.g., Abrahamson and Silva 1996; Kempton and
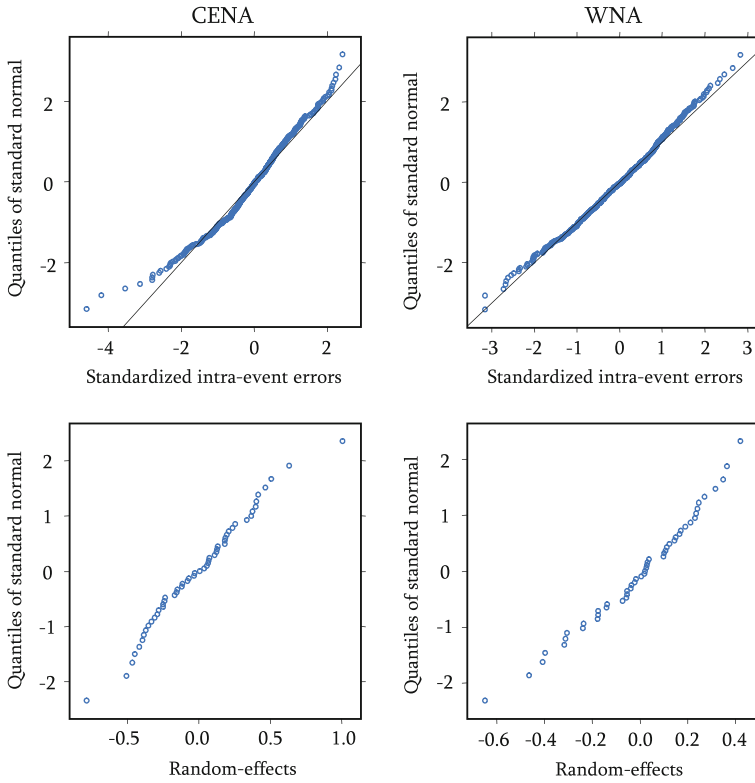
Fig. 5 Normal Q–Q plots of intra-event errors (*top*) and random-effects (*bottom*) for CENA (*left*) and WNA (*right*): D_{5-95}
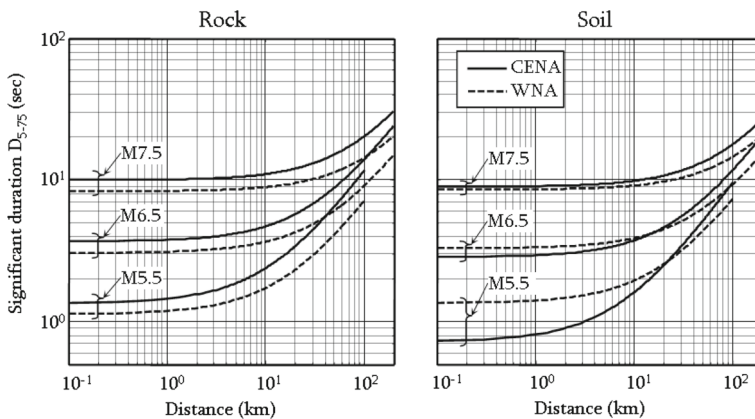

Fig. 6 D_{5-75} comparison of CENA and WNA for rock (*left*) and soil (*right*) sites

Stewart 2006), it is clearly seen that significant duration for CENA increases as site-to-source distance and magnitude increase. Also plotted in Figs. 6 and 7 are the medians for D_{5-75} and D_{5-95} for WNA predicted using Eq. 8 in conjunction with the regression coefficients listed in Table 2. These plots allow the differences in D_{5-75} and D_{5-95} predictions for CENA versus
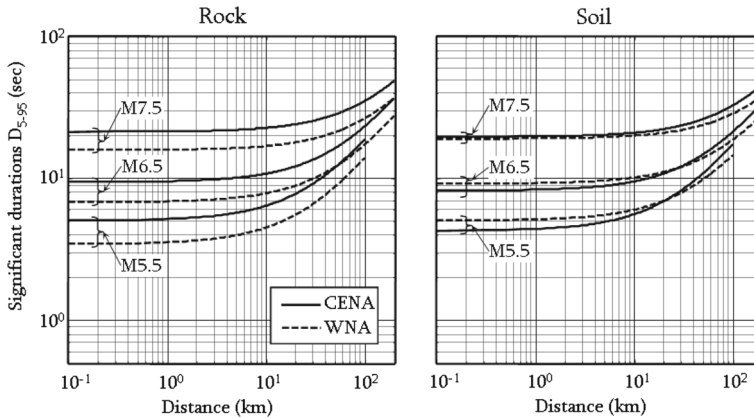
Fig. 7 D_{5-95} comparison of CENA and WNA for rock (*left*) and soil (*right*) sites

WNA to be identified. For rock motions, the significant duration for CENA are systematically longer than those for WNA. In contrast, for soil motions, an opposite trend is observed for small and intermediate earthquake magnitudes (i.e., M5.5 and M6.5) for R < 20 km. However, the differences between rock and soil motion durations are not significant for R < 100 km. Also, contrary to WNA motions, significant durations of rock motions in CENA tend to be slightly longer than those of soil motions. It is not straightforward to explain this inconsistent trend between WNA and CENA motions because significant durations are associated with both amplitude and frequency of ground motions. However, this trend is likely the result of relatively high, high frequency content of the CENA rock motions being significantly filtered out as the motions propagate up through the soil column.

5 Comparison with existing relationships

In the following, comparisons are made among the relationships proposed herein and existing relationships, specifically relationships proposed by Abrahamson and Silva (1996) and Kempton and Stewart (2006). Both of these relationships are for the WNA and were developed using NLME regression analyses. Abrahamson and Silva's model was developed using data from 655 strong ground motion recordings from 58 earthquakes in active shallow crustal regions. The model is expressed as a function of earthquake magnitude, site-to-source distance, and local site conditions. Their model was based on the same site classification system as used in this study (i.e., geomatrix site codes, A and B for rock sites; C and D for soil sites). Also, Abrahamson and Silva used a cut-off distance of 10 km, based on the observed trend that significant durations were independent of the site-to source distance for distances closer than 10 km. Kempton and Stewart used a similar functional form to that of Abrahamson and Silva for developing a "base" model using data from 1,557 recordings from 73 shallow crustal earthquakes. Kempton and Stewart expanded the base model by adding several terms that incorporate near-fault directivity and deep basin effects. Also, local site conditions were represented via the average shear wave velocity in the upper 30 m (V_{S-30}) of a profile, instead of using site classifications.

Similar to Figs. 6 and 7, comparisons of the existing relationships and this study's relationship are shown in Fig. 8 through Fig. 11. The existing relationships for WNA by Abrahamson
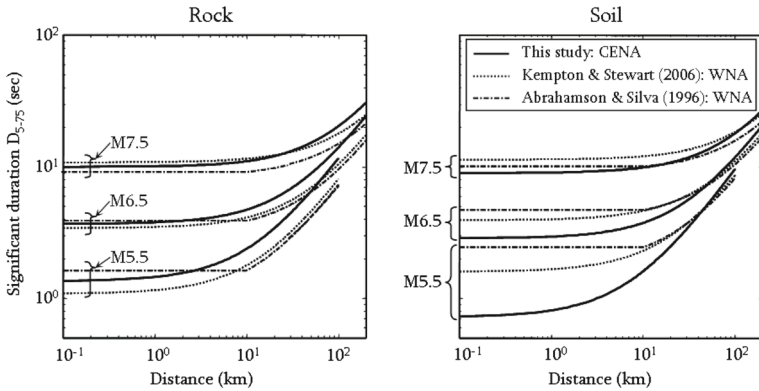
Fig. 8 D_{5-75} comparisons of this study's model for CENA and existing relationships for WNA; the base model was used for Kempton and Stewart (2006)
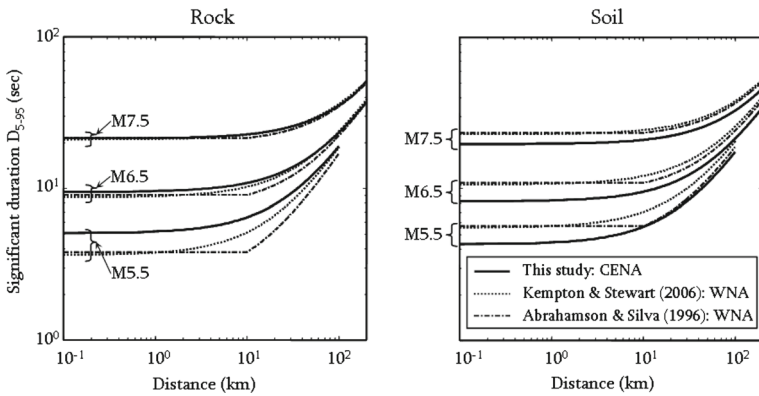

Fig. 9 D_{5-95} comparisons of this study's model for CENA and existing relationships for WNA; the base model was used for Kempton and Stewart (2006)

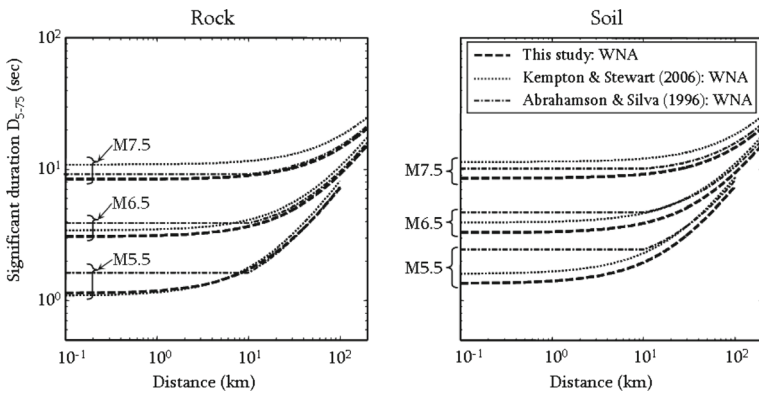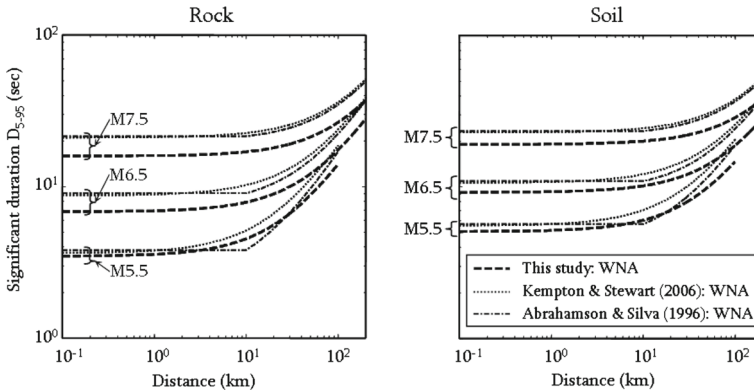**Fig. 10** D_{5-75} comparisons of this study's model for WNA and existing relationships for WNA; the base model was used for Kempton and Stewart (2006)

Fig. 11 D_{5-95} comparisons of this study's model for WNA and existing relationships for WNA; the base model was used for Kempton and Stewart (2006)

Table 3 2011 Mineral earthquake records (CESMD 2012)

No.	Station	Code/ID	Network	R_{epic} (km)
1	North Anna NPP	CW018	–	18.7
		CW026	–	18.7
2	VA Corbin (Fredricksberg Obs)	CBN	NEIC	58.2
3	VA Charlottesville	CVVA	NMSN	53.5
4	VA Reston Fire Station 25	2555	USGS	121.6
5	PA Philadelphia, Drexel Univ	2648	USGS	326.1
6	NY Albany, VA Med	2653	USGS	629.9
7	VT White River Junction VAMC	2655	USGS	787.9
8	VA Pearisburg, Giles County CH	2549	USGS	254.5
9	SC Columbia, VA Hospital	2554	USGS	519.3
10	SC Charleston, Cha Pla Hotel	2544	USGS	603.1
11	SC Summerville, Fire Station	2552	USGS	584.5
12	NY Buffalo, VA Medical Center	2654	USGS	557.3
13	MA Bedford, VA Hospital	2602	USGS	759.6
14	Manchester, VA Medical Center	2652	USGS	787.0
15	MA Boston, Jamaica Plains	2649	USGS	758.0

and Silva (1996) and Kempton and Stewart (2006) are compared with the relationships proposed herein for CENA in Figs. 8 and 9, where the base model is used for the Kempton and Stewart (2006) model. As shown in these figures, there is no systematic trend in the differences between the significant durations for CENA and WNA. It is also shown that the differences in significant durations for CENA and WNA motions are relatively minor. This is consistent with the observations from the comparison of the WNA and CENA relationships shown in Figs. 6 and 7. Additionally, comparisons of WNA motion durations predicted by the existing relationships and this study's relationship are shown in Figs. 10 and 11. As shown in these figures, there is no significant difference between the existing relationships and this study's relationship within the site-to-source distance shorter than about 100 km.
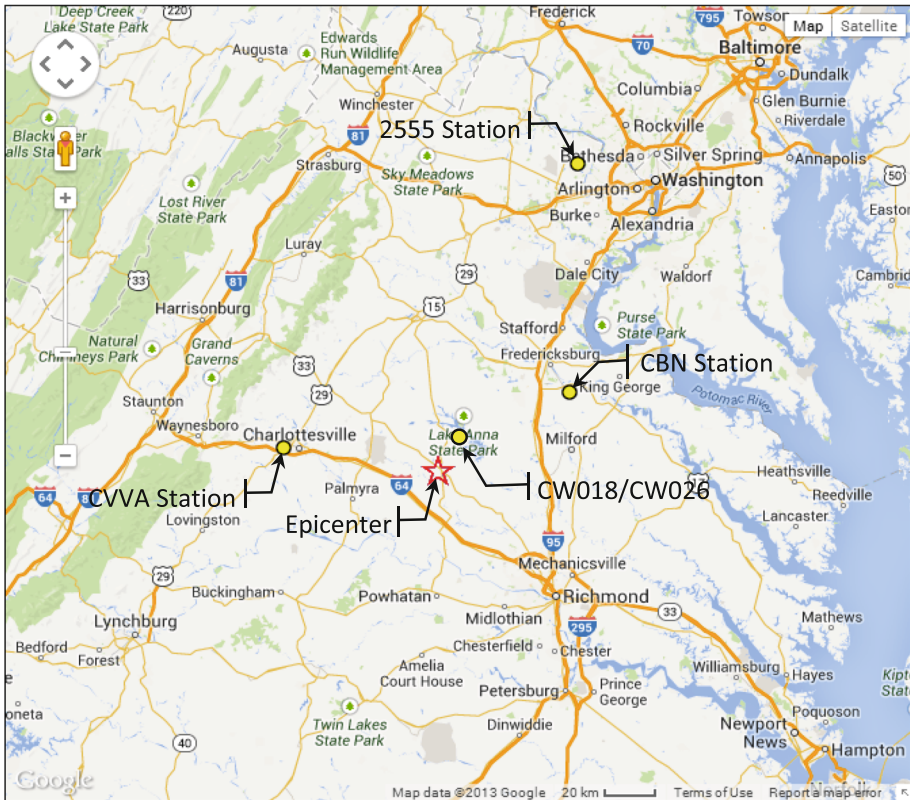
Fig. 12 Locations of the 2011 Mineral earthquake epicenter and the recording stations within 200 km from the epicenter (CESMD 2012); the event was a reverse fault on a north to northeast striking plane dipping to the southeast

6 Comparison with the 2011 Mineral, Virginia earthquake motions

The $M_w 5.8$ Mineral, Virginia earthquake of 23 August 2011 occurred in the Piedmont region of Virginia (Central Virginia Seismic Zone). The epicenter was located about 61 km northwest of Richmond and 8 km south-southwest of the town of Mineral. Its fault mechanism was a reverse slip fault on a north to northeast striking plane dipping to the southeast, and the estimated focal depth was 8.0 km (Chapman 2013). The rupture of the Mineral, Virginia earthquake was comprised of three sub events that occurred over about 1.57 sec with the second slip episode releasing approximately 60 % of the total moment (Chapman 2013).

The significant durations (D_{5-75} and D_{5-95}) of the recorded motions from the mainshock of the 2011 Mineral earthquake are compared with the proposed CENA model. The ground motion records were obtained from the Center for Engineering Strong Motion Data (CESMD 2012), except for those recorded at North Anna nuclear power plant which were obtained directly from Dominion Power. Table 3 lists the 2011 Mineral earthquake motions used herein and their recording stations. Also, Fig. 12 shows the locations of the epicenter and the recording stations within 200 km from the epicenter, where 200 km is the approximately the maximum applicable distance of the proposed relationships.
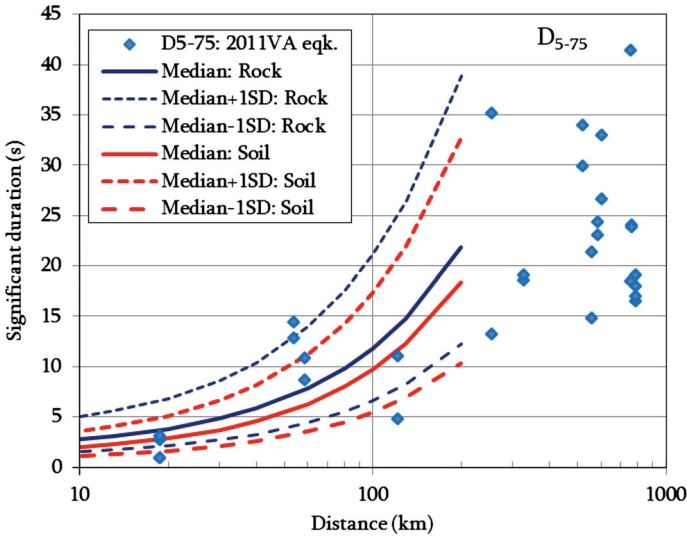
Fig. 13 D_{5-75} comparisons of this study's model for CENA and the 2011 Mineral VA earthquake motions; each pair of the same-distance D_{5-75} data corresponds to two horizontal components recorded at each station
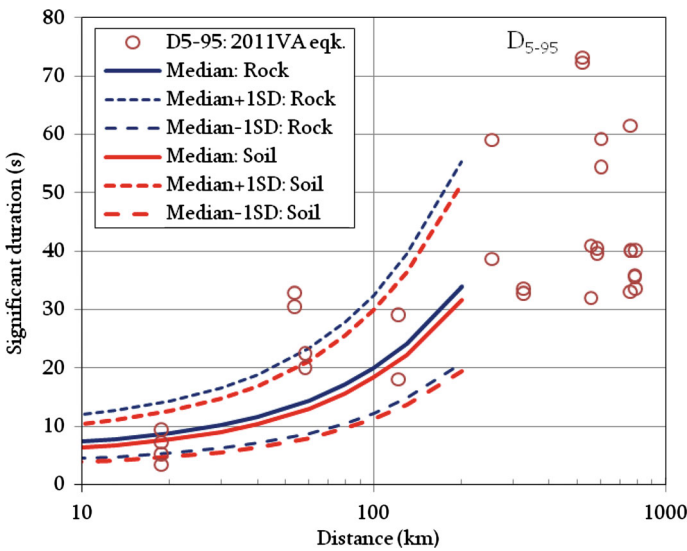

Fig. 14 D_{5-95} comparisons of this study's model for CENA and the 2011 Mineral VA earthquake motions; each pair of the same-distance D_{5-75} data corresponds to two horizontal components recorded at each station

No information of site condition at the recording stations was yet available at the time of the writing of this paper, and thus, the proposed model for both rock and soil sites are plotted for the comparison. Figures 13 and 14 show respectively, the D_{5-75} and D_{5-95} comparisons of both horizontal components of motion recorded at each station during the Mineral earthquake with the proposed CENA model, along with the range of $\pm$ one standard deviation for $M_w5.8$. Note that the proposed model is only plotted up to 200 km, the model's
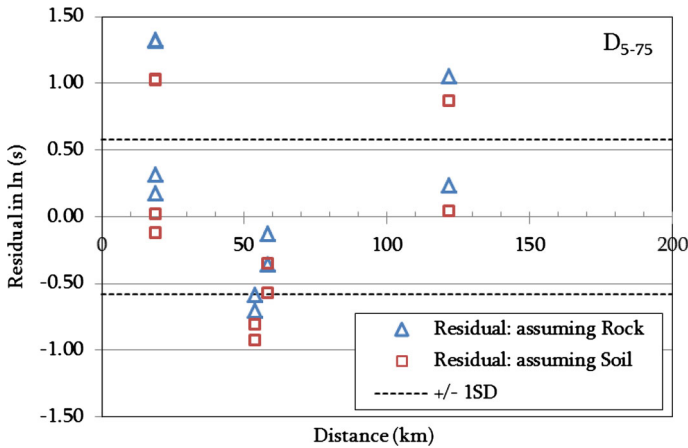
Fig. 15 Residuals and one standard deviation of the proposed model in natural log: D_{5-75}
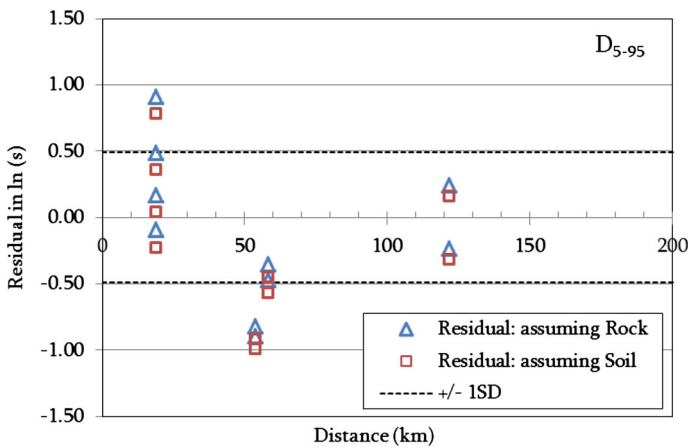

Fig. 16 Residuals and one standard deviation of the proposed model in natural log: D_{5-95}

maximum applicable distance. Figures 15 and 16 show the residuals (i.e., predicted minus observed) for the applicable distance and the model's ± one standard deviation range in a natural log for D_{5-75} and D_{5-95}, respectively. It is noted that the 2011 Mineral earthquake data were not included in the regression analyses to develop the model proposed herein.

The overall trend of the significant duration data from the Mineral earthquake shows that duration generally increase with increasing distance. However, the recorded motions at VA Charlottesville station (CVVA) have considerably longer durations than those from a station at a similar distance (VA Corbin station; CBN). Also in comparison with the proposed CENA model, the significant durations observed at CVVA exceed the 84th percentile durations (median + 1 SD) for both D_{5-75} and D_{5-95}. In addition to possible site effects causing this, CVVA station is located on the footwall side of the fault, while the other stations are on the hanging-wall side. This raises the question of the hanging-wall and footwall effects on strong ground motion durations. To date, there have been few studies investigating the effect of the hanging-wall and footwall on strong motion durations, although several studies

have focused on hanging-wall effects on ground motion amplitude (e.g., Abrahamson and Somerville 1996). Except for the durations observed at CVVA, overall D_{5-75} and D_{5-95} by the proposed CENA model are in reasonably good agreement with those from the 2011 Mineral earthquake.

7 Conclusions

An empirical predictive relationship for significant duration of horizontal strong ground motions in stable continental regions has been developed and presented herein. The empirical significant duration relationship for stable continental regions is based on a total of 310 sets of two horizontal motion records: 14 sets recorded in stable continental regions and the rest being scaled from WNA motions. The moment magnitudes for these motions range from 4.5 to 7.6, and the site-to-source distances range from 0.1 to 199.1 km. Similar to WNA motions, significant durations for CENA motions increased with increasing magnitude and increasing site-to-source distance. Comparing CENA and WNA motion relations from this study, the significant durations for rock motions in CENA were consistently longer than those in WNA, while for soil motions, both CENA and WNA motions were estimated to have similar significant durations. However, no significant differences in the durations for CENA versus WNA were observed within the site-to-source distances shorter than about 100 km. In comparison with the existing relationships for WNA (i.e., Abrahamson and Silva 1996; Kempton and Stewart 2006), the differences in significant durations for CENA and WNA motions were also shown to be relatively minor. Lastly, the proposed CENA model is compared with the recent 2011 Mineral earthquake motions, which shows the predicted significant durations by the proposed model and those from the 2011 Mineral earthquake are in good agreement.

Appendix: Scaling procedure for CENA motions

The scaling procedure used by McGuire et al. (2001) consists of the following computation processes: (1) determination of response spectral transfer function, (2) computation of response spectrum for a given ground motion, (3) determination of target response spectrum, and (4) spectral matching of the time history. A response spectral transfer function was obtained by first using the single-corner frequency point source model (Brune 1970, 1971) to compute smoothed Fourier amplitude spectra (FAS) for both the CENA and WNA. The values of the point source model parameters used are listed in Table 4, where κ is a parameter that represents damping in the shallow crust directly below the site; $\Delta\sigma$ represents the stress drop at the source; Q_0 and n are regional dependent parameters for the frequency dependent quality factor, $Q(f)$; ρ_0 is crustal density in the source region; and β_0 is shear wave velocity of the crust at the source. Next, random vibration theory (RVT) was used to generate response spectra from the FAS (e.g., Boore 1983; Boore and Joyner 1984; Silva and Lee

Table 4 Point source parameters for WNA and CENA motions ([McGuire et al. 2001](#))

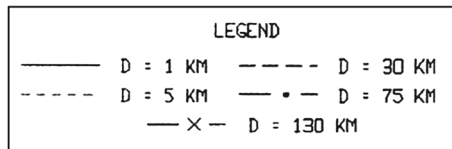|	WNA	CENA
$\Delta\sigma$ (bars)	65	120
κ (s)	0.040	0.006
Q_0	220	351
n	0.60	0.84
β_0 (km/s)	3.50	3.52
ρ_0 (g/cm^3)	2.70	2.60
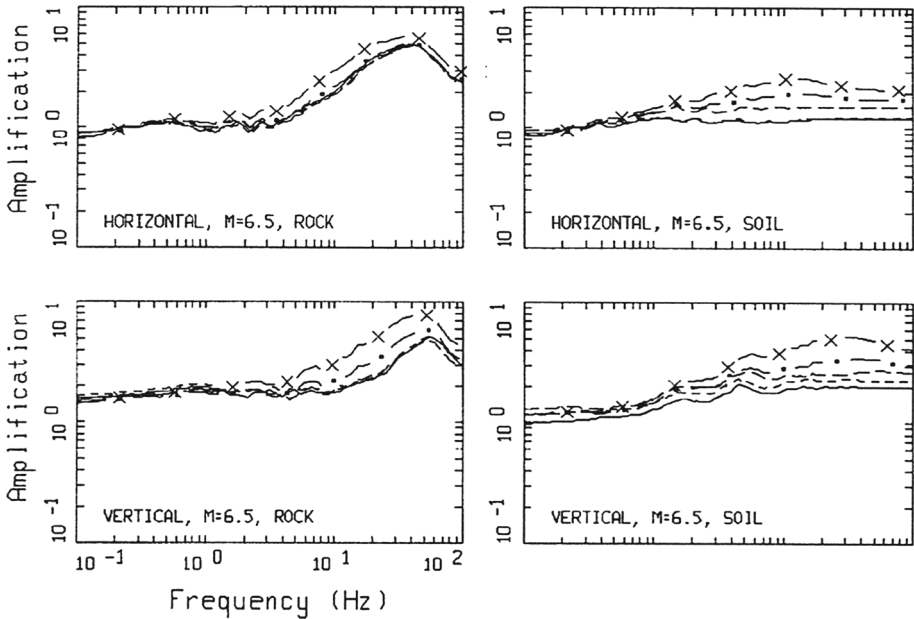
Fig. 17 Response spectral transfer functions for M6.5, rock and soil sites, horizontal and vertical components, and each distance cases (from [McGuire et al. 2001](#))

1987). The ratio of these two response spectra is the spectral transfer function. The response spectral transfer functions were generated for each site condition; horizontal/vertical component; earthquake magnitudes of 5.5, 6.5, and 7.5 (i.e., center value of magnitude bins); and distances of 1, 5, 30, 75, and 130 km. A total 60 different transfer functions were therefore developed. Example transfer functions for M6.5 cases are shown in Fig. 17. The response spectrum (5 % damping) of a WNA "seed" acceleration time history is then computed. Next,

the CENA target response spectrum is obtained by multiplying the "seed" motion's response spectrum by the appropriate response spectral transfer function. Lastly, the "seed" acceleration time history is scaled to match the target CENA response spectrum (Silva and Lee 1987). In the spectral matching process, a sample time interval Δt of 0.005 sec (the corresponding Nyquist frequency is 100 Hz) was used to avoid aliasing effects in the frequency range of interest.

References

Abrahamson NA, Silva WJ (1996) Empirical ground motion models. Report, Brookhaven National Laboratory

Abrahamson NA, Somerville PG (1996) Effects of the hanging wall and footwall on the ground motions recorded during the Northridge earthquake. Bull Seismol Soc Am 86:S93–S99

Bommer JJ, Martinez-Pereira A (1999) The effective duration of earthquake strong motion. J Earthq Eng 3(2):127–172

Boore DM (1983) Stochastic simulation of high-frequency ground motions based on seismological models of the radiated spectra. Bull Seismol Soc Am 73(6A):1865–1894

Boore DM (1986) Short-period P- and S-wave radiation from large earthquakes: Implications for spectral scaling relations. Bull Seismol Soc Am 76(1):43–64

Boore DM, Joyner WB (1984) A note on the use of random vibration theory to predict peak amplitudes of transient signals. Bull Seismol Soc Am 74(5):2035–2039

Brune JN (1970) Tectonic stress and spectra of seismic shear waves from earthquakes. J Geophys Res 75(26):611–614

Brune JN (1971) Correction. J Geophys Res 76(20):1441–1450

Chapman MC (2013) On the rupture process of the 23 August 2011 Virginia earthquake. Bull Seismol Soc Am 103(2A):613–628

CESMD (2012) Center for engineering strong motion data. http://strongmotioncenter.org/

Hanks TC (1979) B-values and omega-gamma seismic source models—implications for tectonic stress variations along active crustal fault zones and the estimation of high-frequency strong ground motion. J Geophys Res 84(NB5):2235–2242

Hanks TC, Kanamori H (1979) A moment magnitude scale. J Geophys Res 84:2348–2350

Husid LR (1969) Características de terremotos. Análisis general. Revista del IDIEM 8, Santiago de Chile, 21–42

Kempton JJ, Stewart JP (2006) Prediction equations for significant duration of earthquake ground motions considering site and near-source effects. Earthq Spectr 22(4):985–1013

Lee J (2009) Engineering characterization of earthquake ground motions. Ph.D. dissertation, University of Michigan, Ann Arbor

McGuire RK, Becker AM, Donovan NC (1984) Spectral estimates of seismic shear waves. Bull Seismol Soc Am 74(4):1427–1440

McGuire RK, Hanks TC (1980) RMS accelerations and spectral amplitudes of strong ground motion during the san-fernando, california earthquake. Bull Seismol Soc Am 70(5):1907–1919

McGuire RK, Silva WJ, Costantino CJ (2001) Technical basis for revision of regulatory guidance on design ground motions: hazard- and risk-consistent ground motion spectra guidelines. US Nuclear Regulatory Commission, Washington, DC

Pinheiro JC, Bates DM (2000) Mixed-effects models in S and S-PLUS. Springer, New York

Program-R (version 2.5.0) A language and environment for statistical computing and graphics. http://www.r-project.org/

Schneider JF, Silva WJ, Stark C (1993) Ground motion model for the 1989 M 6.9 Loma Prieta earthquake including effects of source, path, and site. Earthq Spectra 9(2):251–287

Silva W (1993) Factors controlling strong ground motion and their associated uncertainties. In Dynamic analysis and design considerations for high-level nuclear waste repositories. San Francisco, CA, USA, pp 132–161

Silva WJ, Lee K (1987) WES RASCAL code for synthesizing earthquake ground motions: state-of-the-art for assessing earthquake hazards in the United States. Report 24, US Army Engineering Waterways Experiment Station Vicksburg, MS

Somerville PG, Smith NF, Graves RW, Abrahamson NA (1997) Modification of empirical strong ground motion attenuation relations to include the amplitude and duration effects of rupture directivity. Seismol Res Lett 68(1):199–222

Trifunac MD, Brady AG (1975) Study on duration of strong earthquake ground motion. Bull Seismol Soc Am 65(3):581–626

U.S. Nuclear Regulatory Commission (2007) A performance-based approach to define the site-specific earthquake ground motion. Regulatory Guide 1.208, March